Second-harmonic generation as a DNA malignancy indicator of prostate glandular epithelial cells*

Zhuang Zheng-Fei(庄正飞)[a)], Liu Han-Ping(刘汉平)[a)], Guo Zhou-Yi(郭周义)[a)],
Zhuo Shuang-Mu(卓双木)[b)], Yu Bi-Ying(喻碧英)[b)], and Deng Xiao-Yuan(邓小元)[a)†]

[a)] *MOE Key Laboratory of Laser Life Science, South China Normal University, Guangzhou* 510631, *China*
[b)] *Key Laboratory of Optoelectronic Science and Technology for Medicine, Ministry of Education, Fujian Normal University, Fuzhou* 350007, *China*

(Received 2 January 2009; revised manuscript received 10 October 2009)

This paper first demonstrates second-harmonic generation (SHG) in the intact cell nucleus, which acts as an optical indicator of DNA malignancy in prostate glandular epithelial cells. Within a scanning region of 2.7 μm×2.7 μm in cell nuclei, SHG signals produced from benign prostatic hyperplasia (BPH) and prostate carcinoma (PC) tissues (mouse model C57BL/6) have been investigated. Statistical analyses (t test) of a total of 405 measurements (204 nuclei from BPH and 201 nuclei from PC) show that SHG signals from BPH and PC have a distinct difference ($p < 0.05$), suggesting a potential optical method of revealing very early malignancy in prostate glandular epithelial cells based upon induced biochemical and/or biophysical modifications in DNA.

Keywords: nonlinear microscopy, multiharmonic generation, diagnostic applications of nonlinear optics

PACC: 9575F, 8725, 8170E, 4265, 4262

1. Introduction

Second-harmonic generation (SHG) has attracted wide applications in a variety of biological studies[1−6] as well as in cancer research[7−9] due to its unique properties of no energy loss and coherent preservation of laser light.[10,11]

SHG is an optical phenomenon resulting from the nonlinear polarization of the material:[12]

$$P = \chi^{(1)} \otimes E + \chi^{(2)} \otimes E \otimes E + \chi^{(3)} \otimes E \otimes E \otimes E + \ldots, \quad (1)$$

where P is the induced polarisation vector, E is the electric field vector, $\chi^{(i)}$ is the i^{th}-order nonlinear susceptibility tensor and $\otimes$ represents a combined tensor product and integral over frequencies. SHG is the 2^{nd}-order process related to second nonlinear susceptibility $\chi^{(2)}$, which is introduced by molecular hyperpolarizability β

$$\chi^{(2)} = N_s \langle \beta \rangle, \quad (2)$$

where N_s is the density of molecules and the brackets denote an orientational average, which indicates the need for a non-centrosymmetrical environment requirement of SHG.

More importantly, SHG signals are noted to be tied up with the second-order nonlinear optical susceptibility $\chi^{(2)}$, and the latter physical property is determined by the biochemical and/or biophysical features of the specimen such as its electronic configuration, molecular symmetry, local morphological orientation, molecular alignments and ultrastructures, etc.[13] Furthermore, the biochemical and/or biophysical features in the specimen vary with the progress of the organism and the malignancy.[14,15] The established relationship between SHG signals and biochemical and/or biophysical features in the specimen suggests that SHG signals may be used as an optical indicator for specimen characterization.

The formation of prostate cancer is the growth of malignant glandular epithelial cells in a prostate gland. So far, the prostate-specific antigen test (PSA test) is the most effective tool for prostate disease screening. If PSA is higher than normal levels, which indicates that there are prostate diseases like the infection, benign prostatic hyperplasia (BPH), or malignant changes, cancer. However, it fails to distinguish malignancy from benignancy.[16] A more deter-

*Project supported by the National Natural Science Foundation of China (Grant No. 30470495), the Key Laboratory of Optoelectronic Science and Technology for Medicine, Fujian Normal University.
†Corresponding author. E-mail: xiaoyuandeng@yahoo.co m.cn
© 2010 Chinese Physical Society and IOP Publishing Ltd

minant diagnosis of prostate cancer is prostate biopsy, according to the morphological changes of the histological stained cells by experienced pathologists. Indicators which are prospectively capable of revealing the early modifications by malignancy are to be further explored.

DNA is the earliest biomolecular system that contains the genetic instructions used for the development and functioning of all known living organisms; it has been proven to be an SHG specimen, and this is possibly due to the pseudo-phasematching resulting from its special extended double-helix structure. SHG images of herring sperm DNA in dispersed distilled water under an excitation wavelength of 800 nm have been obtained by C. J. R. Sheppard *et al.*[17]

This suggests that an SHG signal may be used as an optical indicator of understanding biochemical and/or biophysical characteristics occurring in DNA. In this paper, we first demonstrate SHG images of DNA from intact cell nuclei rather than from the dispersed DNA in water. The capability of SHG signals to reveal malignancy changes in DNA is also investigated. Accordingly, two types of cell nuclei are chosen for a comparison, from BPH and prostate carcinoma (PC) tissues in a mouse model C57BL/6, respectively.

2. Experimental setup

The imaging and spectrum system applied in this paper (Fig. 1) employs a mode-locked femtosecond Ti:sapphire laser (Coherent Company) as a laser source (110-fs pulse width, 76-MHz repetition rate and 700–980 nm wavelength-tunable range). An acousto-optic modulator (AOM) is used to control the laser intensity attenuation. The laser is coupled to a confocal scanning microscope (LSM510, Zeiss) and an oil-immersion objective with a numerical aperture (NA) of 1.4 (Plan-Apochromat 63×, Zeiss) is used for microscopic imaging. The near-infrared excitation light is reflected by the main dichroic beam splitter (MDBS) and focused onto the specimen by the objective. The emitted SHG and the fluorescence signals from the specimen are collected by the same objective and go back through the MDBS. The META detector (32 blocks of photomultiplier tube (PMT) are included which cover a total spectral range from 376 nm to 714 nm) is used for imaging as well as the corresponding spectra formation. In front of the META detector, a low pass filter of KP650 (Zeiss) is used to block the excitation light.

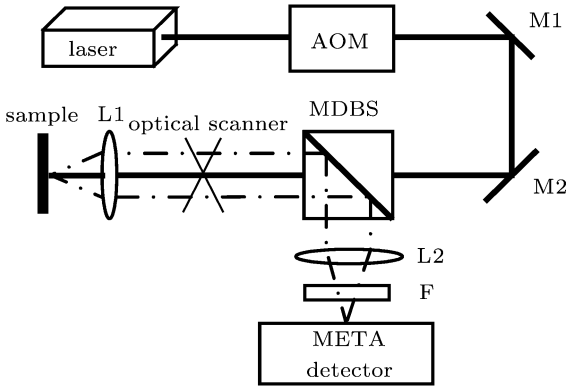


Fig. 1. Laser (Ti:sapphire laser, Coherent Mira 900-F); AOM (acousto-optic modulator); M (mirror); MDBS (main dichroic beam splitter); L1 (oil immersion objective, Plan-Apochromat, 63×, NA=1.4, Zeiss); L2 (lens); F (filter, IR beam block filter, KP650, Zeiss).

3. Materials and methods

The samples used in our study are harvested from inbred strain mouse (C57BL/6). Ten male mice (weighing 18–20 g) purchased from the Laboratory Animal Center (Sun Yat-Sen University, Guangzhou, China) are randomly divided into two groups (five in each) respectively for BPH and PC modeling. Mice manipulations are done in accordance with policies of the Institutional Animal Care and Use Committee (IACUC, 2002). Mouse prostate cancer RM-1 cells, purchased from the Cell Bank of the Chinese Academy of Sciences, are used for PC modeling. They are cultured in Roswell Park Memorial Institute (RPMI-1640 (Gibco)) medium supplemented with fetal bovine serum (FBS) (10%), penicillin (100 U/mL) as well as streptomycin (100 μg/ml), and maintained in a humid chamber (5% CO_2 and 95% O_2) at 37 °C. Cells are then digested with 0.25% pancreatin for subculture, and half of the culture media are refreshed every 3 days before the cell harvest. This is followed by inoculation where rat microglia (RM-1) cells in eugenic condition are washed with D-Hank's solution twice at 37 °C, digested by 0.25% trypsin, centrifuged at 1500 rpm for 5 min and dissociated with RPMI-1640 (containing FBS) into unicelluar suspension (1.3×10^7 cells/ml). BPH model replication:[18] A dosage of testosterone propionate (TP, 5 $mg\cdot kg^{-1}\cdot d^{-1}$) dissolved in soy oil is injected subcutaneously in the ventral skinfold chamber of C57BL/6 mice, once a day for two weeks. The formed prostate tissue blocks are then excised from the body and cryopreserved in a −80 °C refrigerator for slicing. PC model replication:[19] RM-1 unicelluar suspensions

(0.2 ml) are implanted once into the dorsal skinfold chamber of C57BL/6 mice. Once the tumors grow to around 1-cm diameter, solid tumors are excised from the body and preserved as in the above method. The BPH and PC samples are then taken out from the −80 °C refrigerator and set in a −25 °C refrigerator for 6 h in preparation for slicing. Ten slices of 10-μm thickness each are cut sequentially with a cryostat (Leica, CM1850) from each tissue block and are mounted on the slide, fixed in 95% alcohol for 5 min and stained by the standard Van-Gieson (VG) method. The slices are then washed with distilled water, air-dried and overlaid with a cover slip for pathological diagnosis and SHG detection.

4. Experimental results

Samples are confirmed by an experienced pathologist to be BHP and PC tissues, respectively, upon their histological images (Fig. 2).

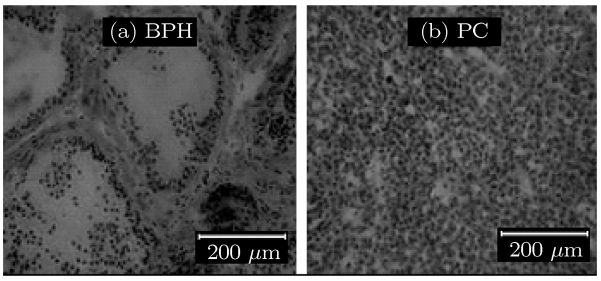


Fig. 2. Characterized BPH and PC slices with VG stain under light microscope (magnification ×400). (a) BPH section demonstrates nodular prostatic hyperplasia in which the glandular lumen become larger than the healthy and pink-stained substance appears. Glandular cells present stratified or pseudostratified columnar epithelium with round nuclei and visible nucleoli inside. (b) PC section demonstrates clustered cells in which nuclei become large and with obviously visible nucleoli.

Figures 3(a) and 3(b) show SHG images of single cell nuclei from BPH and PC cells (scanning area of 10.7 μm×10.7 μm), respectively. Images are formed by an emission spectral range of 409–420 nm under an excitation wavelength of 830 nm and an excitation power of 3 mW (the same conditions are applied in the following experiments). Figure 3(c) demonstrates the spectral range from 376–550 nm of nuclei of BPH and PC within a scanning area of 2.7 μm×2.7 μm (S). Two sharp peaks of the spectra within the spectral region of 400–425 which indicate SHG (verified in the next section) are clearly seen in Fig. 3(c). It is also noticed that the SHG signal produced from the nucleus of the BPH cell is much stronger than that from the PC cell.

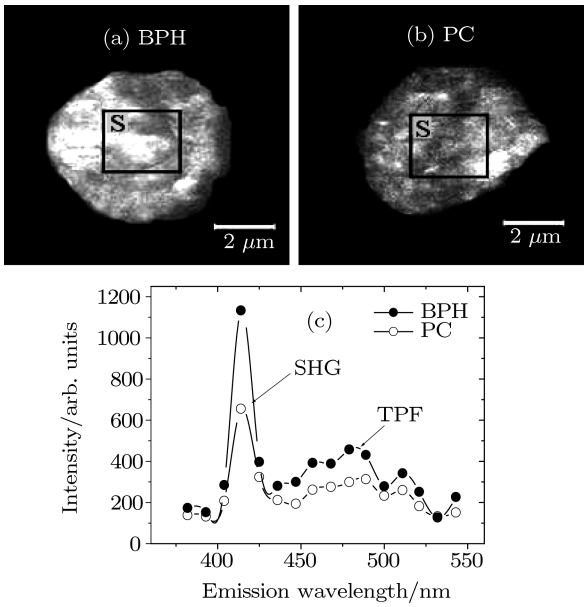


Fig. 3. SHG images and spectra of a single nucleus within a scanning area of 10.7 μm×10.7 μm: (a) SHG image from a nucleus of a BPH cell; (b) SHG image from a nucleus of a PC cell; (c) spectra of nuclei from BPH and PC within a scanning area (S) of 2.7 μm×2.7 μm with spectral range demonstration from 376–550 nm.

To avoid possible effects from the size variation of the nuclei, either from different types of cells or even in the same type of cells, data are all from a fixed small scanning area (S) of 2.7 μm×2.7 μm within the nuclei (shown in Fig. 3). Figure 4 presents the experimental data of the peak intensities of SHG signals based on 405 measurements (204 nuclei from BPH and 201 nuclei from PC, respectively). The corresponding statistical analyses (two independent sample t tests, Statistical Package for the Social Science (SPSS 10.0, SPSS Inc)) show that the SHG peak intensities in the nuclei of BPH cells are on average about 2 times stronger than those from PC cells ($p < 0.05$) (Table 1).

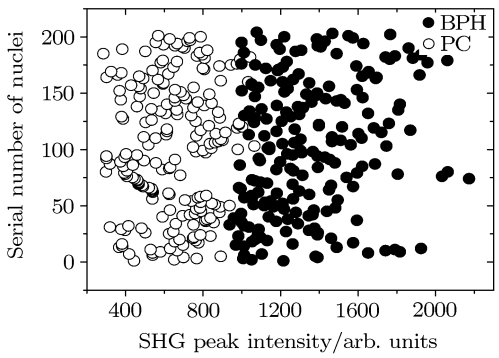


Fig. 4. SHG peak intensities within a scanning area (S) of 2.7 μm×2.7 μm from BPH (204) and PC nuclei (201).

Table 1. Statistical analysis of SHG peak intensities in 405 nuclei within a scanning area (S) of 2.7 μm×2.7 μm from BPH (204 nuclei) and PC (201 nuclei), respectively.

sample	number of nuclei	mean (a.u.)	Se. of mean	t value	2-tail sig.
BPH	204	1344.326	19.963	30.294	$p < 0.05$
PC	201	645.768	130.008		

5. Discussion and conclusions

To verify that the image-based signals and the narrow spectra with sharp peaks (409–420 nm) are SHG, two experiments have been done accordingly. Figure 5(a) demonstrates the tunable peak position of the SHG signals (normalized by their own peak value) as the excitation wavelengths of 790, 800, 820 and 850 nm, respectively. Emission signals are found to be always at half fundamental wavelengths and tunable with excitation wavelengths. Figure 5(b) shows a log–log plot of the SHG peak intensity as the excitation power. The slope of the log–log plot is about 1.9, confirming that SHG satisfies the quadratic dependence on excitation power.

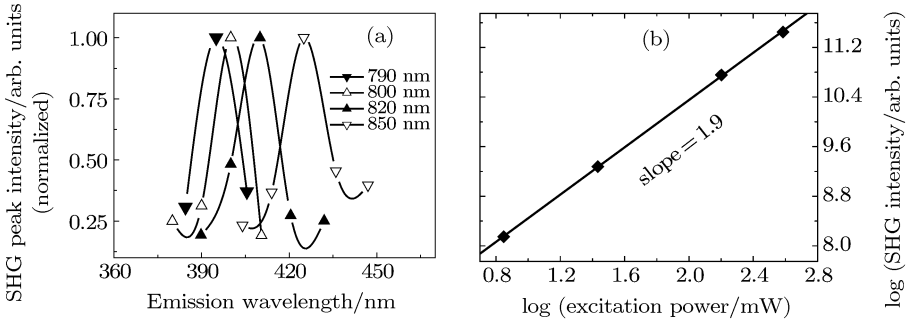


Fig. 5. (a) The SHG peak position along excitation wavelengths of 790, 800, 820 and 850 nm, respectively; (b) log–log plot of SHG peak intensity as a function of the excitation power at an excitation wavelength of 830 nm.

To demonstrate that the origin of the SHG signal is from the native cell nuclei rather than an artifact of the staining procedure, additional experiments dealing with a group of cultured cells instead of cells in tissue have been done. HeLa cancer cells are cultured and used. They keep cultured in Phosphate Balanced Solution (PBS) media in the culture dish. Before scanning, the culture media will be removed, which results in breakage of the membrane of the cells while the cell nuclei are exposed and kept intact. Cells are then excited by an illumination light of 830 nm as for the sliced tissue samples. Images from one single cell are shown in Fig. 6. Figure 6(a) shows the image formed by emission signals between 405 nm to 425 nm. Figure 6(b) shows the transmission image of the cell. By a comparison of these two images, we know for sure that the image in Fig. 6(a) represents the cell nucleus. The corresponding spectrum of this image region (shown in Fig. 6(c)) shows a strong SHG signal peak, which further validates that the cell nucleus is the origin of the contributor of the SHG signal.

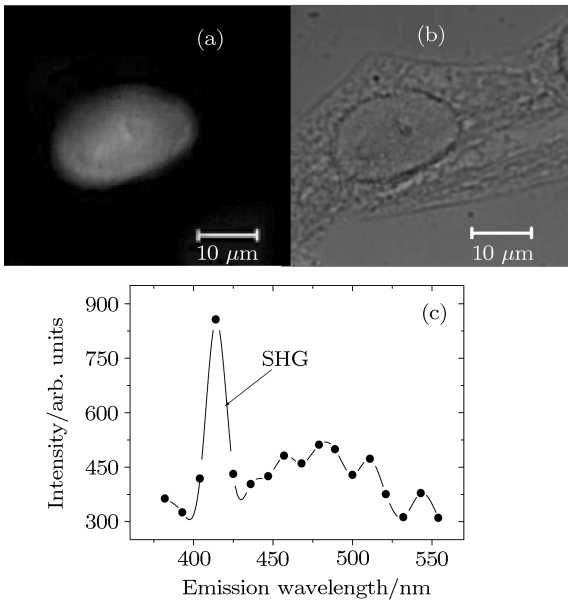


Fig. 6. Images and spectra of a single HeLa cancer cell (with broken cell membrane because PBS culture media has been removed from the cell before scanning): (a) SHG image (405 nm–425 nm) from a single HeLa cancer cell; (b) transmission image of a single HeLa cancer cell; (c) spectra of a single HeLa cancer cell (376–550 nm).

Van Gieson's (VG) staining is adopted here for two reasons. One is the location requirement of target nuclei under the microscope, and the second is because VG staining is a common histological staining method to distinguish cell nuclei from surrounding extracellular fibres. The nuclear counter-stain is chosen to be Weigert haematoxylin (WH) in our VG staining. The stain haematoxylin is not a dye, but develops colouring properties on oxidation to haematin. This substance haematin has little or no affinity for tissue elements and requires an inorganic ion (here it is iron) to act as a mordant. Facing outward and holding the negative charge, we find that the phosphoric group in the two bonds of the DNA double helix specially combines with WH that carries a positive charge by iron bonds,[20] making the nuclei identifiably blue. Apparently, the staining process does not interfere with the basic double helix structure in DNA as the prerequisite of producing SHG as demonstrated by the experimental results. Our experimental results of generated fluorescence by haematoxylin on DNA are weak, which is consistent with the previous semiquantitative evaluation of fluorescence intensity in chromatin stained with iron haematoxylin under green exciting light (545 nm) in paraffin sections of rat embryos (18 days old).[21]

In conclusion, in this paper, we first demonstrate that SHG from DNA in cell nuclei is a powerful optical indicator of malignancy in prostate glandular epithelial cells, offering a possible optical method for biochemical and/or biophysical feature-based early malignancy detection. Our experiments also provide clues for further malignancy mechanism exploration.

Acknowledgements

The authors gratefully thank Prof. Chen Jian-Xin, Ms. Wu Su-Lian, and Ms. Liu Nong-Rong for their helpful assistance.

References

[1] Campagnola P J and Loew L M 2003 *Nat. Biotechnol.* **21** 1356
[2] Zoumi A, Yeh A and Tromberg B J 2002 *Proc. Nat. Acad. Sci.* **99** 11014
[3] Moreaux L, Sandre O, Charpak S, Mireille B D and Mertz J 2001 *Biophys. J.* **80** 1568
[4] Deng X Y, Wang X J, Liu H P, Zhuang Z F and Guo Z Y 2006 *J. Biomed. Opt.* **11** 024013
[5] Zhu X F, Zhou L, Zhang D and Gong X F 2005 *Chin. Phys.* **14** 1594
[6] Fan T B, Zhang D, Zhang Z, Ma Y and Gong X F 2008 *Chin. Phys.* B **17** 1674
[7] Sacconi L, D'Amic M, Vanzi F, Antolini R, Biagiotti T, Olivotto M and Pavone F S 2005 *J. Biomed. Opt.* **40** 24014
[8] Brown E, Mckee T, Ditomaso E, Pluen A, Seed B, Boucher Y and Jain R K 2003 *Nat. Med.* **9** 796
[9] Deng X Y, Williams E D, Thompson X, Gan X and Gu M 2002 *Scanning* **24** 175
[10] Boyd R W 2003 *Nonlinear Optics* (New York: Academic Press) p. 89
[11] Zipfel W R, Williams R M and Webb W W 2003 *Nat. Biotech.* **21** 1369
[12] Campagnola P J and Loew L M 2003 *Nat. Biotech.* **21** 1356
[13] Shen Y R 1989 *Nature* **337** 519
[14] Rebecca M, Williams R M, Warren R, Zipfel W R and Webb W W 2005 *Biophys. J.* **88** 1377
[15] Guo Y C, Savage H E, Liu F, Schantz S P, Ho P P and Alfano R R 1999 *Proc. Nat. Acad. Sci.* **96** 10854
[16] Bowsher W snd Carter A 2006 *Challenges in Prostate Cancer* (Oxford: Blackwell Publishing) p. 63
[17] Gauderson R, Lukins P B and Sheppard C J R 2001 *Micro.* **32** 685
[18] Mahapokai W and Schalken J A 2000 *Prostate Cancer Prostatic Dis.* **3** 28
[19] Prerna S and Nicole S A 1999 *Oncogene* **18** 5349
[20] Prento P 1993 *Histochemistry* **99** 163
[21] Apgar J M, Juarranz A, Espada J, Villanueva A, Canete M and Stockert J C 1998 *Journal of Microscopy* **191** 20